PASSIVE LOAD ALLEVIATION BY NONLINEAR MOUNTING OF AIRFOILS IN 2-DOF MODELS

D. Hahn*†, M. Haupt*†

* Cluster of Excellence SE^{2}A - Sustainable and Energy-Efficient Aviation, Technische Universität Braunschweig, Germany

† Institute of Aircraft Design and Lightweight Structures, Technische Universität Braunschweig, Hermann-Blenk-Str. 35, D-38108 Braunschweig, Germany

Abstract

A two degree of freedom (2-DOF) heave-pitch aeroelastic model with nonlinear spring attachments is set up and used to investigate the load alleviation capabilities of a new passive load alleviation concept. The concept is to exploit the nonlinear behaviour of structural wing components to trigger a deformation which reduces loads once a certain load level is reached. The deformation is a wing twist reducing the angle of attack. This structural nonlinear behavior is introduced into the 2-DOF model by implementing springs, which become weaker at a critical displacement, as attachment. Analyses with stationary loads and dynamic gust encounters at different flight conditions and different weights of the wing section are made. The best alleviation is achieved in stationary cruise and in long gusts and low wing mass. In slow flight the alleviation capability is reduced because of less aerodynamic pitching moment. The alleviation capabilities are reduced in short gusts and with high wing masses due to inertia.

Keywords

passive load alleviation, structural nonlinearity, heave-pitch-model

1. INTRODUCTION

Reducing the weight plays a major role in the development of new efficient aircraft. Less weight leads to less fuel consumption and less emissions of pollutants. This is an important contribution necessary for reaching the goals of Flightpath 2050.

The wing structure contributes significantly to the structural weight of an aircraft. Wings are designed to withstand maneuver and gust loads up to 2.5 g. For normal operations a load factor of 2.5 g is not necessarily needed. If it can be ensured, that a load factor of 2.5 g can not occur during a maneuver or gust encounter, the wing can be designed for a lower load level. This allows for a lighter structure. The limitation of the maximum aerodynamic load which can physically occur is achieved with load control or load alleviation.

There are different approaches to achieve load alleviation. Active load alleviation uses sensors and control surfaces or other actuating measures to adapt the wing to a gust. Modern airliners already use active load alleviation utilizing their primary control surfaces [1]. Current research covers forward looking sensors using LIDARs [2] to better predict necessary actuations of the load alleviation system. Research is also made on advanced actuation such as using piezoelectric actuation in combination with compliant structures to create a morphing smooth wing [3].

Passive load alleviation on the other hand does not use sensors and actuators. Therefore such components do not contribute to the weight of the aircraft. Also system failures like electrical problems do not affect passive methods. Passive approaches include e.g. aeroelastic tailoring. This is a technique to design a wing with bending torsion coupling. This is done by using the anisotropic stiffness of fiber composites to change the orientation of the stiffest direction out of the span wise direction. Bending torsion coupling induces twisting, which lowers the angle of attack in the outer wing when the wing is bend up [4]. Another method to reach bending torsion coupling is a “Z-Beam” spar [5]. Other approaches feature hinged wingtips, either unrestrained [6] or attached with a nonlinear negative stiffness spring device [7]. A different approach for dynamic load events focuses on the application of dampers at wing struts, which are able to limit the wing root bending moment when eigenmodes are excited from a gust [8].

The aim of the author’s project within the cluster of excellence SE^{2}A (**S**ustainable and **E**nergy-**E**fficient **A**viation) is to exploit significant structural nonlinearities such as local buckling for passive load alleviation. The tailored use of nonlinearities allows for a nonlinear onset or increase of the load alleviating wing deformation beginning at a critical load. The deformation modes are wing twist and camber changes. It is an extension of classical aeroelastic tailoring into

doi: 10.25967/550238

the nonlinear regime. The basic idea of this concept is sketched in fig. 1.

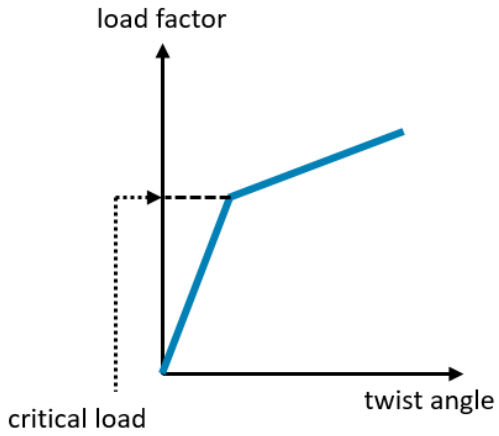

FIG 1. Sketch of the basic concept for the use of nonlinear behavior

This contribution shows studies with a two-dimensional two degree of freedom (2-DOF) aeroelastic model, in which the attachment springs for heave and pitch are nonlinear. Additional heave-pitch coupling terms are introduced. The load alleviation capabilities of the envisioned concept are evaluated with this model. It is also used to find an appropriate stiffness design and consider dynamic effects. A sketch of the 2-DOF model with highlighted nonlinearities, i.e. the dependency on heave and pitch, is depicted in fig. 2.

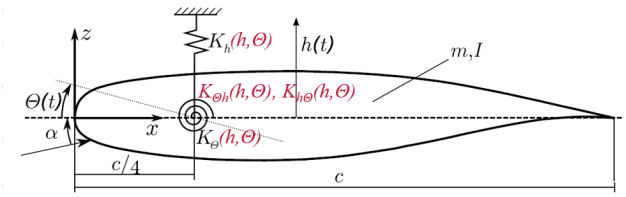

FIG 2. 2-DOF Model with mounting nonlinearities in red. Sketch without nonlinearities based on [9].

The model setup is covered more in depth in section 2. Section 3 presents stationary analyses for the stiffness design and maneuver loads. Dynamic gust encounters are shown in section 4. Section 5 concludes the paper.

2. METHODS

The aeroelastic 2d Model with 2 DOF and nonlinear mounting is developed using the coupling environment *ifls* [10], *DLR-TAU Code* [11] for the fluid model and a custom python-based structural model. After an introduction to *ifls*, the models and methods which are then coupled together are presented.

2.1. Coupling environment *ifls*

The coupling environment *ifls* [10] is an in-house software developed at the Institute of Aircraft Design and Lightweight Structures of TU Braunschweig. It is an coupling environment for fluid-structure interaction which may also include heat transfer. The different domains structure and fluid are calculated by separate solvers. *ifls* couples them together and takes care of grid interpolation and the solution process of the coupled equilibrium. The architecture is schematically displayed in fig. 3. The control code is written by the user and defines the iterative coupling process. The interface between the separate solver and the control code is the co-process. It translates commands like solving a timestep to the necessary creation of solver input and run commands of the solver. A new solver can be made available for *ifls* by introducing an appropriate co-process.

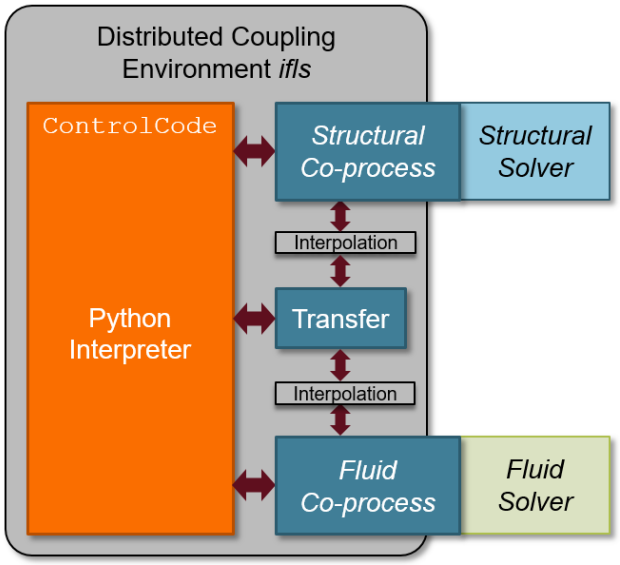

FIG 3. Architecture of the coupling environment *ifls*. Based on [12]

2.2. Fluid model

The fluid model for the 2-DOF aeroelastic model is a computational fluid dynamics (CFD) model using *DLR-TAU Code* [11]. It represents a quasi 2D section of the supercritical DLR-F15 airfoil, which is used in the reference aircraft of the cluster of excellence SE^2A [13]. The compressible Euler equation is used instead of the Reynolds Averaged Navier Stokes (RANS) equation for computational time. The grid has 4408 cells and no special boundary layer treatment since this is not required for the Euler equation. It is depicted in fig. 4. The chord length is 2.3 m and the depth of the section is 1 m.

Deformations from the fluid-structure interaction are introduced into the grid using the grid deformation tool of the *DLR-TAU Code*, which receives the commands from *ifls*.

In the dynamic gust simulations the gust is introduced using the disturbance velocity approach (DVA), which is included with the *DLR-TAU Code*.

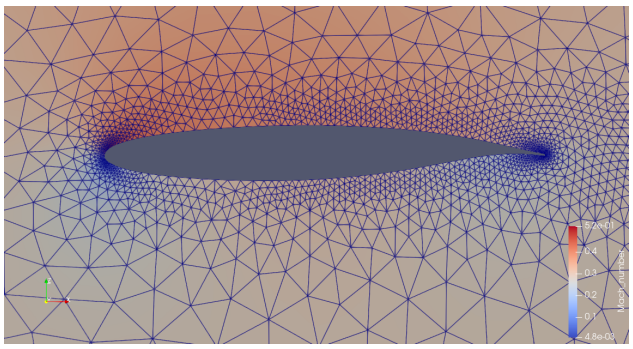

FIG 4. Grid of the DLR-F15 airfoil with mach number contour at Ma = 0.3

2.3. Structural model

The structural model is a custom python-based code. It calculates the response of a two mass oscillator with the degrees of freedom heave h and pitch Θ (refer to fig. 2) to a given force, static or dynamic. In the static case it solves the equilibrium equation

$$\mathbf{F}_R = \mathbf{F}_{ext} \tag{1}$$

with the restoring force

$$\mathbf{F}_R = \mathbf{K}\mathbf{U} \tag{2}$$

and external force $\mathbf{F}_{ext}$ representing aerodynamic forces. Both force vectors have the corresponding components translational force F and moment M:

$$\mathbf{F} = \begin{bmatrix} F \\ M \end{bmatrix} \tag{3}$$

The displacement vector

$$\mathbf{U} = \begin{bmatrix} h \\ \Theta \end{bmatrix} \tag{4}$$

has the degrees of freedom as components. The stiffness matrix

$$\mathbf{K} = \begin{bmatrix} K_h & K_{h\Theta} \\ K_{\Theta h} & K_\Theta \end{bmatrix} \tag{5}$$

has the components translational stiffness K_h, rotational stiffness K_Θ and the coupling terms $K_{\Theta h}$ and $K_{h\Theta}$, which create a restoring moment induced by heave and a restoring translational force induced by pitch.
If the components of the stiffness matrix are constant, the system is linear and can be solved directly by inverting the stiffness matrix:

$$\mathbf{U} = \mathbf{K}^{-1}\mathbf{F}_{ext} \tag{6}$$

However, since the components of the stiffness matrix are functions of the displacement vector, the system is nonlinear and needs to be solved iteratively using the Newton-Raphson method:

$$\mathbf{U}_{k+1} = \mathbf{U}_k - \mathbf{K}(\mathbf{U}_k)^{-1} \cdot (\mathbf{F}_k(\mathbf{U}_k) - \mathbf{F}_{\mathbf{ext}}) \tag{7}$$

In the dynamic case inertia and viscous forces are added to the equilibrium:

$$\mathbf{M}\ddot{\mathbf{U}}(t) + \mathbf{K}\mathbf{U}(t) = \mathbf{F}_{ext}(t) \tag{8}$$

with time t, the mass matrix

$$\mathbf{M} = \begin{bmatrix} m & S \\ S & I_y \end{bmatrix} \tag{9}$$

with mass m, static moment S and moment of inertia I_y. Each timestep is solved with the Newmark method [14], which is a predictor - corrector method. Due to the nonlinear stiffness matrix the dynamic Newmark method is embedded in an iterative Newton-Raphson Method [15] to create new predictors based on the result of the former iteration, until the method has converged in the time step.
A Co-process with the necessary interface methods to *ifls* is adapted based on [9].

2.4. Stationary aeroelastic model

This section briefly describes the calculation procedure defined with the control code for *ifls* in this model. The stationary model calculates at least two aeroelastic equilibrium states. The first one is the reference state with predefined angle of attack. Other states have a changed fluid angle of attack $\Delta\alpha$. An aeroelastic equilibrium is a state, where the aerodynamic forces and the structural restoring forces, which both are functions of the displacement, are equal:

$$\mathbf{F}_{aero}(\mathbf{U}) = \mathbf{F}_R(\mathbf{U}) \tag{10}$$

The equilibrium is iteratively solved by solving the fluid model and subsequently solving the structural model with the resulting aerodynamic force. The resulting displacement is then used as new boundary condition for the fluid model in the next iteration. To improve convergence, the displacement is relaxed using the Aitken relaxation method for vector equations [16], before it is used in the next iteration.
The reference state is iteratively trimmed to a defined effective angle of attack. The effective angle of attack

$$\alpha_{eff} = \alpha + \Theta(\alpha_{eff}) \tag{11}$$

is the angle between the airflow and the chord. It is a result of the fluid angle of attack α, which is the angle between the airflow and the fixed chord of the initial state, and the pitch angle Θ (refer to fig. 2). The pitch angle Θ is a function of the lift, which is a function of α_{eff}.
Trimming the reference state for a defined effective angle of attack α_{eff} is necessary to begin the calcu-

lation with defined initial lift, like e.g. cruise condition. Otherwise, different cases with different stiffness values at the same fluid angle of attack α would have a different pitch Θ and subsequently a different effective angle of attack α_{eff}. This would create difficulties in comparing the results. To trim the state an aeroelastic equilibrium is calculated and a new fluid angle of attack for the next iteration is defined from the results:

$$\alpha_{i+1} = \alpha_i + k \cdot (\alpha_{eff,target} - \alpha_{eff}) \tag{12}$$

Factor k is 1 by default. It can be adjusted in case of convergence problems. If the angles oscillate around the target angle, $k < 1$ can prevent the angles from overshooting. When the angles approach the target slowly, $k > 1$ can accelerate convergence. However, this factor is not automatically changed in the code but has to be adjusted manually. In this study convergence is achieved for all cases with $k = 1$.
In all other states, which are compared to the reference state, a change of the fluid angle of attack $\Delta\alpha$ is applied. No trimming for a specific lift is done, because it is the target to observe the pitch and subsequent lift reaction of the structural design to the changed airflow $\Delta\alpha$.
In the stationary case the fluid model can be simplified, because moment and lift are functions of only the effective angle of attack for a given flight condition. It is not necessary to complete a full CFD calculation for each equilibrium iteration. Prior to the stationary aeroelastic analysis, a pure CFD calculation is made to create a data set for moments and forces for different angle of attacks. This data is interpolated for the use in the stationary model.

2.5. Dynamic aeroelastic model

The dynamic aeroelastic model for gust encounter simulations uses mostly the same procedures as the stationary model. For the initial condition a trimmed stationary equilibrium is calculated like in sec. 2.4. In the time loop, equilibrium states are calculated for each timestep, using the dynamic methods of the fluid and structure solvers to account for inertia effects. The coupling is a strong coupling, which means that the equilibrium states are solved iteratively like in sec. 2.4.
In the dynamic model it is not possible to use the simplified fluid model. The reason is the influence of instationary aerodynamics and the gust position on moments and forces. This means that they are not only functions of the effective angle of attack for a given flight condition. Therefore CFD calculations with the *DLR-TAU Code* are solved in each iteration step.

3. STATIONARY ANALYSES

The stationary model is used to set up the nonlinear stiffness selection and evaluate the load alleviation for stationary loads, e.g. maneuver loads. To ensure maneuverability, passive load alleviation strong enough to prevent any significant lift increment should not be implemented in the whole wing. Maneuver load alleviation is therefore applied in the outer area of the wing to shift the load to the inner wing, which reduces the root bending moment.

3.1. Flight conditions

Two flight conditions are derived from the SE^{2}A medium range reference aircraft flight profile [13]. They cover the begin of climb and begin of cruise. Both are with high mass because the fuel is not yet consumed. Therefore the lift requirement is high as well. The conditions differ in speed, lift coefficient and altitude. The cases are defined in tab. 1

parameter	unit	climb case	cruise case
altitude	m	1500	10600
density	kg/m^3	1.058	0.383
mach number	-	0.297	0.78
true airspeed	m/s^1	99.3	231.5
mass	kg	71950	70640
lift coefficient	-	0.791	0.399

TAB 1. Flight conditions for case climb and case cruise

3.2. Nonlinear stiffness concept

The aim of the nonlinear stiffness concept is to achieve an increased downward pitch when the load surpasses the 1g condition.
In the 2-DOF model, pitch down is the result of an aerodynamic pitching moment, as well as of an increased internal moment. In cases, in which the downward aerodynamic pitching moment increases with increasing angle of attack, the desired nonlinear pitch down can be realized with a nonlinear weakening torsional spring for the attachment. However, in many cases this prerequisite for the behavior of the aerodynamic pitching moment is not fulfilled. The behavior depends on the airfoil, transonic airspeed and the position of the attachment.
For a more universal applicability the use of coupling terms is required. The coupling terms represent structural behavior like bending torsion coupling. This paper does not consider how the coupling is technically realized in real structures. The calculation results can be interpreted as guidance for the requirements of the structural behavior for real structures. Even though not included in this contribution, the authors also investigate the structural design of wingbox segments with nonlinear bending tosion coupling [17].
The coupling terms as defined in eq. 5 create additional forces and moments in the structure, which are added to the restoring forces. A moment is induced by heave, and a force is induced by pitch. With coupling terms the required increasing downward

moment at increasing lift can be realized more independently from the aerodynamic behavior. The limitation to that independence is that the coupling in real structures can not be infinitely large. Without nonlinearities this bending torsion coupling is like classical aeroelastic tailoring. A downward pitch at increasing load and therefore some load alleviation is realized. However, in this state it is linear.
The desired nonlinear increase of pitch down can then be achieved by making both attachment springs nonlinear. The stiffness of both springs needs to drecrease increasing deformation. In this study the springs have two stiffness levels. In order to keep the function continuous both levels are connected by a very steep ramp instead of a jump at the critical displacement. This behavior is sketched in fig. 5. The

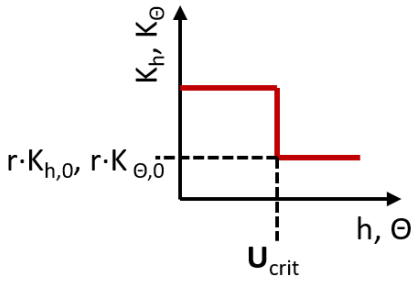

FIG 5. Schematic behavior of the spring stiffnesses.

functional principle of this modification is that increasing lift leads to heave and also to pitch down due to the coupling term. When the critical displacement is reached, the translational spring becomes less stiff and subsequently the heave will increase stronger with lift. Due to the coupling the same holds true for the induced moment and corresponding pitch down. When the torsional spring becomes less stiff, the induced moment has a stronger effect on the pitch.

3.3. Selection of the stiffness properties

The selection of the stiffness values is made with the cruise case as design point. The reason for that is, that in the cruise case the aerodynamic downward pitching moment is higher than in the climb case. This is due to the transonic speed with a compression shock on the airfoil near the trailing edge. Using this case as design point is conservative, because the aerodynamic pitching moment and the induced structural moment are added together. If the design would be made for the climb case with reduced aerodynamic pitch moment, the total moment in the cruise case could be too high for the torsional spring. This means that it can not keep the pitch limited, resulting in torsion divergence. This risk can be avoided by using the case with high aerodynamic pitching moments as design point. However, due to less aerodynamic pitching moment in the climb case, the achieved pitch down can not be as strong in the climb case as in the cruise case.

The stiffness values are set to achieve deformations of 70 mm and -2.4° at 1g load. These displacements are in the same order of magnitude as the displacements in [9]. The coupling terms are already included in the deformations and set in a way, that the induced moment is in the same order of magnitude as the aerodynamic pitching moment. The stiffness reduction factor r is set such that the lift coefficient has a small positive slope with increasing $\Delta\alpha$. If the slope was negative, higher angle of attacks would not only lead to a reduction of the additional lift, but of the total lift. This could result in the loss of control in an aircraft. A value of $r = 0.4$ is found to fulfill these requirements for the selected stiffness properties. The factor is applied to the stiffnesses, when the corresponding displacement is higher than factor 1.04 of the 1g displacement. A list of the stiffness values is given in tab. 2. This property selection is used in this study, however the model can be easily adopted to different stiffness properties.

parameter	unit	value
K_h	N/m	150000
K_Θ	Nm/rad	500000
$K_{\Theta h}$	Nm/m	-100000
$K_{h\Theta}$	N/rad	-100000
r	-	0.4

TAB 2. Stiffnesses of the 2-DOF Model

3.4. Stationary loads at the design point (cruise)

Results for the stationary model in cruise, which is the design point, are shown in fig. 6. The lift coefficient C_L shows the desired nonlinear behavior and increases only 16 % at $\Delta\alpha$ = 3°. Without nonlinear springs C_L increases by 97 %, as indicated by the red line. The load increment in the nonlinear structure is thus reduced by 83.5 % at this $\Delta\alpha$ compared to the linear structure. This is a significant stationary load reduction, that is useful in the outer area of the wing. Fig. 7 shows the increased pitch down, which is the reason for the load alleviation. It has to be noted, that discussed here is the additional load alleviation created by the nonlinearity. The linear elastic structure already has some load alleviation compared to a fixed structure due to the bending torsion coupling. This coupling is visible by the negative slope of the pitch Θ in the linear structure.

3.5. Stationary loads at off-design (climb)

A strong load alleviation can be designed at the design point (sec. 3.4). Due to different aerodynamic pitching moments the load alleviation is less effective in other design points. Fig. 8 and fig. 9 show the behavior in the climb case.
Because of the different speed, different angle of attacks are required for the same lift. The lift increments of the nonlinear system are therefore evaluated

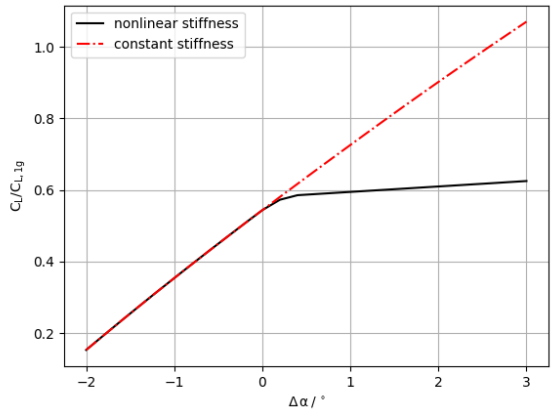

FIG 6. Change of Lift coefficient C_L due to a change of $\Delta\alpha$ at the design point for linear and nonlinear springs.

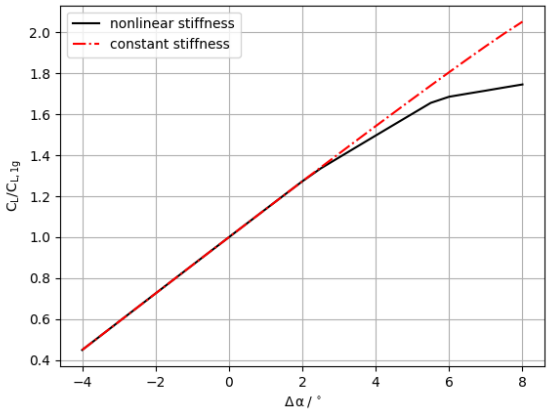

FIG 8. Change of Lift coefficient C_L due to a change of $\Delta\alpha$ at off-design for linear and nonlinear springs.

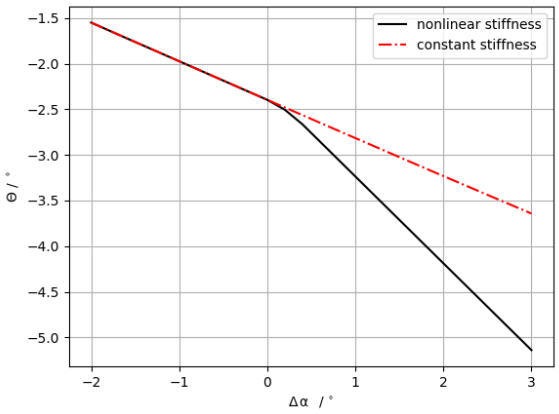

FIG 7. Change of pitch Θ due to a change of $\Delta\alpha$ at the design point for linear and nonlinear springs.

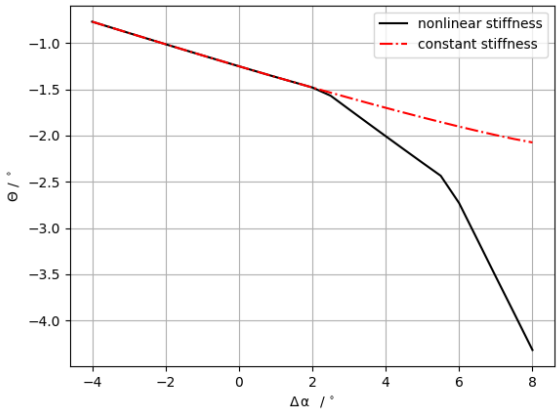

FIG 9. Change of pitch Θ due to a change of $\Delta\alpha$ at off-design for linear and nonlinear springs.

at an defined lift increment of the linear system. This allows comparison of the lift increment reduction between the design point and the off-design point in the nonlinear system. In the design point the lift increases by 97% at $\Delta\alpha = 3°$ in the linear structure. In the climb case, this lift increment in the linear system is found at $\alpha = 7.3°$. The C_L increment at this $\Delta\alpha$ in the nonlinear system is 72 %. This is a reduction of the lift increment by 25.7 % compared to the linear system.

Reasons for the reduced alleviation effectiveness compared to the design point are less aerodynamic pitching moment and higher requirements for the change of the angle of attack for lift changes due to the reduced speed . Additionally, since there is less pitching moment, the pitch at which the torsional spring becomes weaker is reached at higher angles than the weakening of the translational spring. This effect can be seen by the two kinks the figures 8 and 9. Even though the alleviation is not as effective as in the design point, there is still the useful alleviation of 25.7 % at $\Delta\alpha = 7.3°$. However, this kind of passive load alleviation is significantly influenced by the flight condition.

The use of the Euler equation in this study amplifies the difference between the flight conditions compared to the difference in a RANS calculation. In a stationary RANS calculation made for comparison, the compression shock in the transonic regime is shifted towards the leading edge. This results in reduced aerodynamic pitching moments compared to Euler. The difference between the aerodynamic pitching moment in cruise and in climb is expressed by the amplification factor. Using Euler the amplification factor is 3.7. Using RANS it is only 2.9. The reduced difference between the flight conditions using RANS is beneficial for the effectiveness of the load alleviation mechanism in off-design points.

4. DYNAMIC ANALYSES

To assess the influence of mass inertia and instationary aerodynamics on the load alleviation, dynamic analyses are required.

4.1. Gust encounter cases

Vertical gust encounters are selected for the dynamic simulations, because gusts lead to changes of the angle of attack in short time frames. According to certification specification CS 25.341 [18] the gusts are simulated using a 1-cos shape with a gust wavelength in the range from 18 m to 214 m. In this study, the two mentioned boundaries of the wavelength range and a vertical velocity of 10.2 m/s in cruise condition are selected. The two gust shapes are depicted in fig. 10.

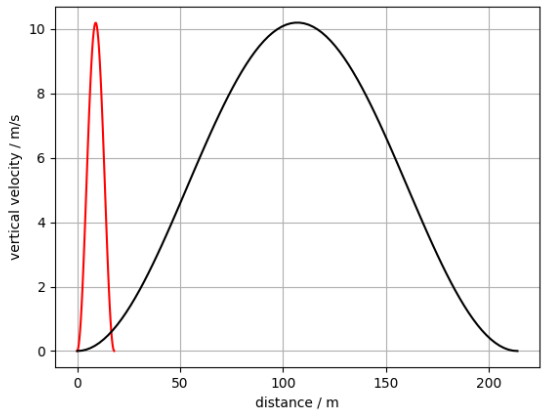

FIG 10. Vertical gusts selected for the simulation

For the assessment of inertia influences, different masses are used in the structural model of the wing section. For the calculation of static moments and moments of inertia, a uniform mass distribution is applied. The masses vary between 1 kg and 1000 kg, which extends the range a real wing would have. A 1 m section of a real wing is estimated to have a weight of 200-600 kg, depending on the fuel level. This estimation is made based on the wing mass of the reference configuration [13]. The stiffness properties are the same as in the stationary case (sec. 3.3).

4.2. Results of the dynamic analyses

Results for C_L of the dynamic calculations of the short gust are shown in fig. 11 with the lowest and the largest analyzed masses. In the 1000 kg case there is no difference between nonlinear and linear behavior and hence no additional load alleviation. The reason is the slow reaction of the structure, which can be noticed in the plot of Θ in fig. 12. The maximum pitch down and the difference between linear and nonlinear structure take place after the gust has already passed the airfoil.

In the case of low mass the reaction of the structure reacts immediately. This results in a significantly increased absolute value of Θ in the nonlinear structure compared to the linear structure. With the fast reaction, the lift increment is reduced by 45 %.

Also, the maximum load in the linear structure is lower in the low mass case than in the high mass case. The reason is also the influence of inertia.

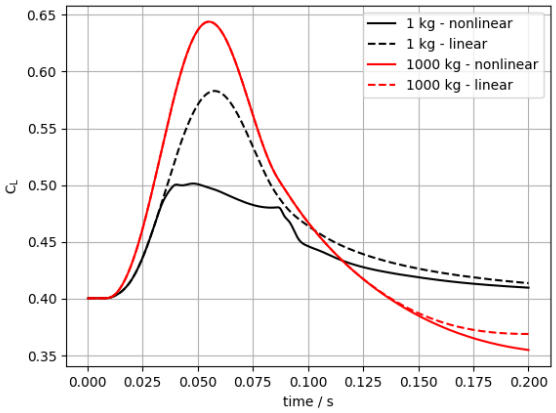

FIG 11. Lift coefficient C_L in a 18 m gust encounter with linear and nonlinear springs

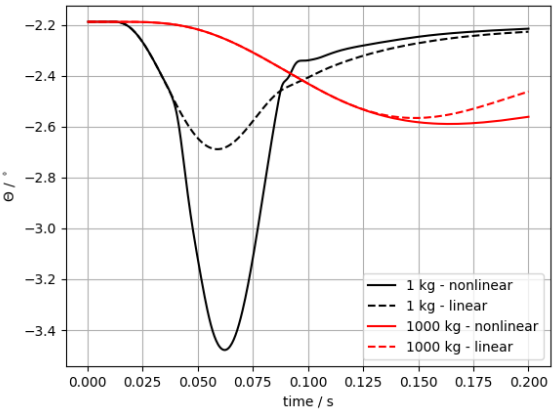

FIG 12. Pitch angel Θ in a 18 m gust encounter with linear and nonlinear springs

Because of the bending torsion coupling the linear elastic structure has some pitch down and load alleviation. The immediate reaction of the lighter structure allows for the peak of the downward pitch to be at the time of gust peak. In the heavy structure, the peak of the downward pitch is reached after gust, which temporarily results in slightly lower lift than in cruise condition.

In the longer gust, the structure has more time to react. As visible in fig. 13 the time is sufficient for the heavy structure to achieve a reduction of 15 % lift increment at its highest peak. The light structure has a lift increment reduction of 67 %, as it reacts almost instantaneously.

The lift of the heavy structure temporarily drops significantly below cruise lift. The reason is, that due to the inertia the structure pitches further down than the stationary equilibrium (fig. 14). The stationary equilibrium is at 4.25° pitch down. This value is reached by the light structure with small inertia. The pitch difference in the heavy structure is high because the eigenfrequency is in the same order of magnitude as the inverse gust duration. The gust excites eigenmodes of the aeroelastic system, which

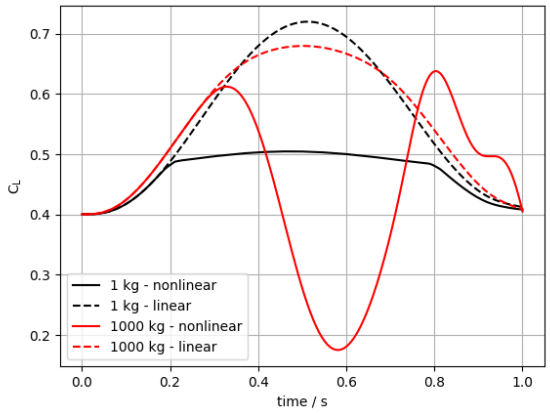

FIG 13. Lift coefficient C_L in a 214 m gust encounter with linear and nonlinear springs

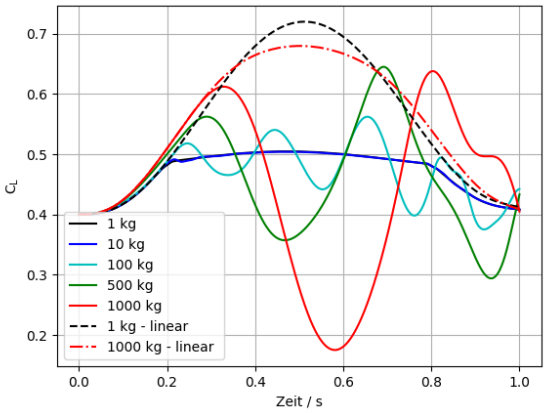

FIG 15. Lift coefficient C_L in a 214 m gust encounter with more mass cases

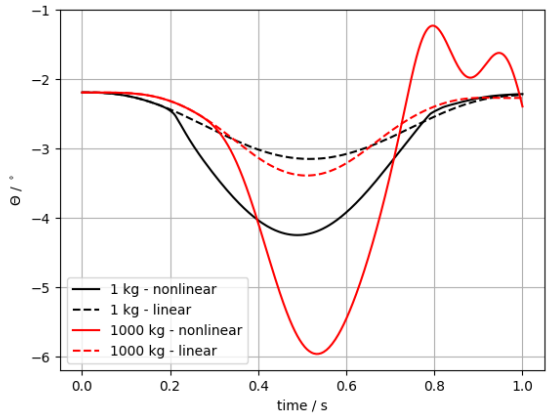

FIG 14. Pitch angel Θ in a 214 m gust encounter with linear and nonlinear springs

can be seen for C_L with more different mass values in fig. 15. With all masses eigenmodes are excited. The amplitude is smaller at higher frequencies. Since low mass leads to a high frequency, the oscillations have low amplitudes and are barely visible for the light cases with 1 kg and 10 kg. At slower frequencies in the vicinity of the gust length, the oscillations rise until the gust significantly decays. At the end of the gust all found oscillations decay. High oscillation amplitudes limit the maximum achieved load alleviation. This shows, that when designing a real structure care has to be taken that tuned gusts do not produce larger oscillations. They must not be too large the structure to withstand. Additionally, large oscillations prevent the load alleviation from being effective, because the downward pitch is temporarily reduced.

5. CONCLUSIONS

This paper presented a 2-DOF aeroelastic model, which is used to investigate nonlinear stiffness for passive load alleviation. The airfoil is attached with a translational and a rotational spring and coupling terms are added in the stiffness matrix. One coupling term introduces a structural moment under heave motion. When the airfoil is lifted by an increasing angle of attack, the coupling makes it pitch down which reduces the additional lift. The investigated load alleviation concept makes use of structural nonlinearities to increase this pitch down at and above a critical load. This is realized by making the springs become less stiff at a critical displacement. When the translational spring becomes weaker, it results in more heave and due to the coupling more pitch down moment. When the torsional spring becomes less stiff, the pitch down moment can rotate the wing further.

This model was analyzed in stationary and dynamic simulations. For stationary loads at the design flight condition very effective load reduction can be designed with this principle. This study does not cover, how the nonlinearity and bending torsion coupling values can be realized in a real structure. However, the authors presented investigations on the structural design of wingbox segments with nonlinear structural behavior in [17].

In off-design flight conditions the load alleviation effectiveness is decreased, because there is less aerodynamic pitching moment to support the pitch down. The design should be made for the case with highest aerodynamic pitching moments to prevent unstable behavior in a case with higher moment.

Dynamic gust encounter simulations show a significant dependency from inertia effects. Longer gusts and smaller weights have more effective load alleviation than shorter gusts and higher weights. Depending on the eigenfrequencies of the system and the gust length, a gust can excite oscillations, which decay after the gust. Analyzing the dynamic reaction to tuned gusts is therefore necessary in the design of such load alleviation mechanisms.

It was shown that load alleviation based on nonlinear structural behavior in principle works in a fluid-structure interaction calculation. In the 2-DOF model, the nonlinear stiffness matrix is artificially designed to tune the structure for effective load alleviation. This

provides guidance for the structural requirements of real structures. Future studies will cover full 3D wings with a finite element structure model, in which the nonlinear behavior is calculated based on the real structure.

ACKNOLEDGEMENTS

We would like to acknowledge the funding by the Deutsche Forschungsgemeinschaft (DFG, German Research Foundation) under Germany's Excellence Strategy **EXC 2163/1** - Sustainable and Energy Efficient Aviation - **Project ID 390881007**

Contact address:

daniel.hahn@tu-braunschweig.de

References

[1] C. D. Regan and C. V. Jutte. Survey of Applications of Active Control Technology for Gust Alleviation and New Challenges for Lighter-weight Aircraft. NASA, Dryden Flight Research Center, Edwards, California, USA, 2012.

[2] N. Fezans and H.-D. Joos. Combined Feedback and LIDAR-Based Feedforward Active Load Alleviation. In *AIAA Atmospheric Flight Mechanics Conference*, Reston, Virginia, 2017. American Institute of Aeronautics and Astronautics. DOI: 10.2514/6.2017-3548.

[3] A. C. Henry, G. Molinari, J. R. Rivas-Padilla, and A. F. Arrieta. Smart Morphing Wing: Optimization of Distributed Piezoelectric Actuation. *Journal of Intelligent Material Systems and Structures*, 57(6):2384–2393, 2019. DOI: 10.2514/1.J057254.

[4] W. R. Krüger, J. Dillinger, R. de Breuker, and K. Haydn. Investigations of passive wing technologies for load reduction. *CEAS Aeronautical Journal*, 10(4):977–993, 2019. DOI: 10.1007/s13272-019-00393-2.

[5] O. Stodieck. Tech-insight: Aeroelastic tailoring of wings using a Z-beam concept. University of Bristol, 2019.

[6] A. Castrichini, V. Hodigere Siddaramaiah, D. Calderon, J. E. Cooper, T. Wilson, and Y. Lemmens. Nonlinear Folding Wing-Tips for Gust Loads Alleviation. In *56th AIAA/ASCE/AHS/ASC Structures, Structural Dynamics, and Materials Conference*, page 4, Reston, Virginia, 2015. American Institute of Aeronautics and Astronautics. DOI: 10.2514/6.2015-1846.

[7] A. Castrichini, J. E. Cooper, T. Wilson, A. Carrella, and Y. Lemmens. Nonlinear Negative Stiffness Wing-Tip Spring Device for Gust Loads Alleviation. In *15th Dynamics Specialists Conference*, page 1701, Reston, Virginia, 2016. American Institute of Aeronautics and Astronautics. DOI: 10.2514/6.2016-1574.

[8] C. P. Szczyglowski, S. A. Neild, B. Titurus, J. Z. Jiang, J. E. Cooper, and E. Coetzee. Passive gust loads alleviation in a truss-braced wing using integrated dampers. In *International Forum on Aeroelasticity and Structural Dynamics, IFASD*, 2017.

[9] K. Lindhorst, M. Haupt, and P. Horst. Efficient surrogate modelling of nonlinear aerodynamics in aerostructural coupling schemes. *AIAA Journal*, 52(9):1952–1966, 2014. DOI: 10.2514/1.J052725.

[10] M. Haupt, R. Nies, R. Unger, and P. Horst. Computational aero-structural coupling for hypersonic applications. In *9th AIAA/ASME Joint Thermophysics and Heat Transfer Conference*, page 3252, 2006.

[11] D. Schwamborn, T. Gerhold, and R. Heinrich. The DLR TAU-code: Recent applications in research and industry. In *European Conference on Computaional Fluid Dynamis ECCOMAS CFD 2006*, 01 2006.

[12] M. Müller, M. Woidt, M. Haupt, and P. Horst. Challenges of Fully-Coupled High-Fidelity Ditching Simulations. *Aerospace*, 6(2), 2019. DOI: 10.3390/aerospace6020010.

[13] S. Karpuk and A. Elham. Conceptual Design Trade Study for an Energy-Efficient Mid-Range Aircraft with Novel Technologies. In *AIAA Aerospace Sciences Meeting 11–15 January 2021*, 2021.

[14] N. M. Newmark. A Method of Computation for Structural Dynamics. *Journal of the Engineering Mechanics Division*, 85(3):67–94, 1959. DOI: 10.1061/JMCEA3.0000098.

[15] E. Chatzi and G. Abbiati. The Finite Element Method for the Analysis of Non-Linear and Dynamic Systems. Lecture.

[16] B. M. Irons and R. C. Tuck. A version of the aitken accelerator for computer iteration. *International Journal for Numerical Methods in Engineering*, 1(3):275–277, 1969. DOI: https://doi.org/10.1002/nme.1620010306.

[17] D. Hahn and M. Haupt. Potential of the nonlinear structural behavior of wing design components for passive load alleviation. In *Deutscher Luft- und Raumfahrtkongress DLRK 2020*, 2020.

[18] EASA. Certification Specifcations CS25 Amendment 17. Accessed 23.08.2021.